Inorganica Chimica Acta 579 (2025) 122561

Contents lists available at ScienceDirect

Inorganica Chimica Acta

journal homepage: www.elsevier.com/locate/ica

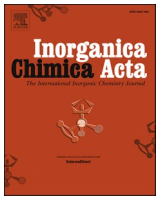

Luminescent Ru(II) complexes based on functionalised 1,10-phenanthroline derivatised ligands towards bioconjugated probes

Alexandra R. Ibbott, Paula Miquel Fosco, Deemah M. Alenazy, Simon J.A. Pope *

School of Chemistry, Main Building, Cardiff University, Cardiff CF10 3AT, Cymru/Wales, UK

ARTICLE INFO

Keywords:
Phenanthroline
Ruthenium
Bioconjugation
Luminescence

ABSTRACT

A series of photoluminescent, heteroleptic $[Ru(bipy)_2(\mathbf{L^n})](PF_6)_2$ (2,2′-bipyridine = bipy; $\mathbf{L^n}$ = 1,10-phenanthroline derivative) analogues have been prepared. Within the series of complexes the structural variation is provided by the ancillary ligand, $\mathbf{L^n}$, which is based upon a 5-substituted 1,10-phenanthroline species. The synthesis of the ligands was achieved in two steps from 5,6-epoxy-5,6-dihydro-1,10-phenanthroline allowing a range of different morpholine, piperazine and piperidine derivatives to be attached to the 1,10-phenanthroline core at the 5-position. Furthermore, the synthetic utility of the piperazine derivative ($\mathbf{L^1}$) was demonstrated by bioconjugating a cholesteryl moiety to the ligand (yielding $\mathbf{L^8}$). Following complexation, the isolated Ru(II) complexes show classical ^{3}MLCT characteristics with phosphorescent emission at 605–610 nm.

1. Introduction

Polypyridyl complexes of Ru(II) are ubiquitous in coordination chemistry [1]. Building from pioneering work several decades ago, such complexes still attract substantial attention due to the ongoing discovery and breadth of their potential applications. The attractive optoelectronic properties of $[Ru(N^{\wedge}N)_3]^{2+}$ complexes (where N^N = polypyridine variants) coupled with a detailed understanding of fundamental electronic [2], photochemical [3] and photoredox [4] behaviours has continued to attract the interest of researchers from diverse backgrounds, including photocatalysis [5]. The biological applications of these complexes also continue to develop in extensiveness: building from light switch DNA binders [6], through to photo-cytotoxic species [7] in photodynamic [8] or photoactivated therapy [9], and potential therapeutics [10], as well as cellular imaging probes [11]. The demands of the applications has led to an incredible diversity in ligand structures, which are often based upon 2,2′-bipyridine or 1,10-phenanthroline species and variations thereof.

1,10-Phenanthroline (phen) is one of the most common ligand structures used in coordination chemistry since the 1950s [12] and is particularly common in Ru(II) studies. As a ligand class, the chemistry of phen has been extensively reviewed, including a very recent focus on different synthetic approaches for functionalisation (especially the reactivity at the [2,9], [3,8], [4,7] and [5,6] positions) that encompasses the current state of the art [13]. As noted by Queffelec et al., functionalisation, either through convergent (functionalised precursors to phen) or divergent synthetic strategies (building from phen), can impart desirable properties upon the ligand and subsequent metal complexes.

Reactions at the [5,6] positions of phen (Scheme 1) are very attractive as this allows functionalisation to occur without sterically inhibiting the chelating ability of the phen nitrogens. Different synthetic approaches can introduce substituents and/or increase the conjugation of the pi-system. One of the most common approaches is to form the diketone (known as the 5,6-dione) requiring both oxidising and acidic conditions in the treatment of phen [14]. The phen 5,6-dione species is a very convenient precursor for targeting highly conjugated and rigid ligands such as dipyrido[3,2-a:2′,3′-c]phenazine (dppz) [15], as well as imidazo[4,5-*f*][1,10-phenanthroline] species [16]; these two classes of compound have seeded, in their own right, a huge diversity of ligands available through simple variations in approach.

In comparison, the chemistry of 5,6-epoxy-5,6-dihydro-1,10-phenanthroline [17] (Scheme 1) is far less reported. As well as a viable ligand in its own right [18], the functionality of this species affords a different reactivity and reports have shown that a range of nucleophiles (amine, thiol [19], azide, cyanide) can ring-open the epoxide, initially giving a 6-substituted, 5,6-dihydro-1,10-phenanthrolin-5-ol species. The dehydration mediated re-aromatisation of the ring, to reform an authentic 1,10-phenanthroline species, is not always spontaneous and depends upon the nature of the nucleophile/substituent. For example, reaction of the

* Corresponding author.
E-mail address: popesj@cardiff.ac.uk (S.J.A. Pope).

https://doi.org/10.1016/j.ica.2025.122561
Received 19 November 2024; Received in revised form 20 January 2025; Accepted 21 January 2025
Available online 24 January 2025

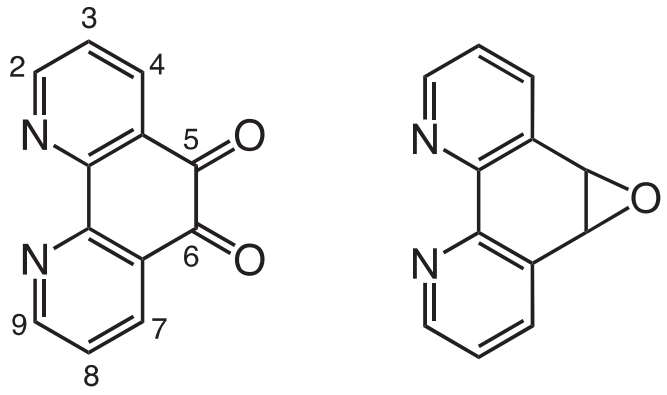

Scheme 1. A comparison of two phen structures promoting functionalisation at the [5,6] positions: 1,10-phenanthroline-[5,6]-dione (left) and 5,6-epoxy-5,6-dihydro-1,10-phenanthroline.

epoxide with KCN will give 5-cyano-1,10-phenanthroline [20], whereas reaction with an amine (R_2NH) generally will not, requiring an additional treatment with NaH to induce re-aromatisation (see Scheme 2) [21]. Therefore 5,6-epoxy-5,6-dihydro-1,10-phenanthroline is a valuable entry point to mono-functionalised phen ligands, including examples focussed upon bioconjugation [22], and bioimaging probes [23], sensing [24], polymetallic arrays for water relaxometric agents [25], polymer networks [26], and 5-azido species for click chemistry [27].

The basis of the current work was therefore to further explore ligand derivatives of 1,10-phenanthroline via the chemistry of 5,6-epoxy-5,6-dihydro-1,10-phenanthroline and demonstrate their viability in photoluminescent Ru(II) complexes. In doing so we were able to develop a range of monosubstituted 5-amino-1,10-phenanthroline derivatives by utilising different morpholine, piperidine and piperazine variants (Scheme 3). In the case of the 5-piperazinyl species, further functionalisation was demonstrated by reaction with a cholesteryl derivative thus showing the viability of this approach to areas of study where bioconjugation is required.

2. Experimental

^{1}H, $^{13}C\{^{1}H\}$, $^{19}F\{^{1}H\}$ NMR spectra were recorded on an NMR-FT Bruker 300, 400 or 500 MHz spectrometers and recorded in $CDCl_3$, CD_3CN, CD_3OD, $(CD_3)_2CO$ or $(CD_3)_2SO$. ^{1}H and $^{13}C\{^{1}H\}$ NMR chemical shifts (δ) were determined relative to residual solvent peaks with digital locking and are given in ppm. Coupling constants are quoted in Hz. High-resolution mass spectra were obtained on a Waters QTOF instrument by the staff at Cardiff University. UV–Vis studies were performed on a Shimadzu UV-1800 spectrophotometer as MeCN or MeOH solutions. Photophysical data were obtained on MeCN solutions using a JobinYvon–Horiba Fluorolog spectrometer fitted with a JY TBX picosecond photodetection module. The pulsed source was a Nano-LED configured for 295 nm output operating at 1 MHz. Luminescence lifetime profiles were obtained using the JobinYvon–Horiba FluoroHub single photon counting module and the data fits yielded the lifetime values using the provided DAS6 deconvolution software. Quantum yield measurements were obtained on aerated MeCN solutions of the complexes using $[Ru(bipy)_3](PF_6)_2$ in aerated MeCN as a standard (Φ = 0.018) [28].

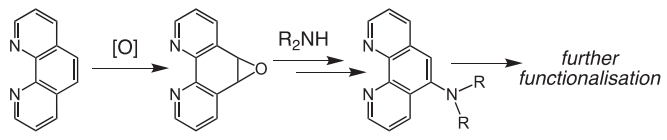

Scheme 2. The general synthetic route explored for the 1,10-phenanthroline ligands described herein.

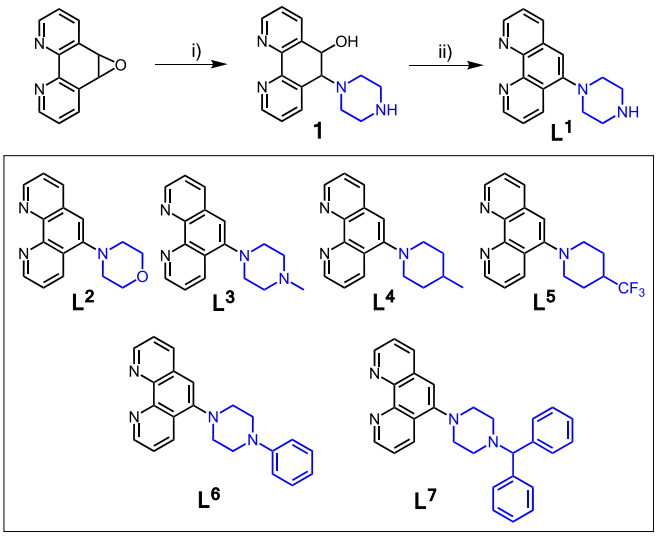

Scheme 3. Top: Exemplar synthetic route to $\mathbf{L^1}$ via its precursor, **1**, with the additional target ligands shown inset. Reagents and conditions: i) 3 eq. piperazine, EtOH, heat; ii) NaH, dry THF, heat.

2.1. Synthesis of 6-(piperazin-1-yl)-5,6-dihydro-1,10-phenanthrolin-5-ol. (1)

5,6-epoxy-5,6-dihydro-1,10-phenanthroline (0.250 g, 1.3 mmol) and piperazine (0.330 g, 3.9 mmol) were combined in ethanol (25 mL). The reaction mixture was heated to reflux under a nitrogen atmosphere for 16 h. The reaction was then cooled to room temperature and the solvent removed under vacuum. The resultant off-white residue was retrieved through filtration and washed with toluene (3 × 10 mL) and diethyl ether (10 mL) to yield a cream powder (0.337 g, 93 %). ^{1}H NMR (300 MHz, $(CD_3)_2SO$, 298 K) δ_H: 8.62 (1H, d,J_{HH} = 1.6 Hz), 8.60 (1H, d,J_{HH} = 1.6 Hz), 7.97 (1H, dd, J_{HH} = 7.7 Hz, 0.9 Hz), 7.91 (1H, dd, J_{HH} = 7.7 Hz, 1.2 Hz), 7.44 (1H, d [],J_{HH} = 4.7 Hz), 7.41 (1H, d,J_{HH} = 4.7 Hz), 4.99 (1H, d,J_{HH} = 7.7 Hz), 3.84 (1H, d,J_{HH} = 7.7 Hz), 3.17 (4H, app. s), 2.69 (1H, s), 2.66 (4H, app. s) ppm. $^{13}C\{^{1}H\}$ NMR (101 MHz, $(CD_3)_2SO$, 298 K) δ_C: 151.1, 149.9, 148.8, 148.6, 136.9, 136.7, 134.8, 132.3, 124.0, 123.9, 67.6, 67.3, 50.7, 46.7, 46.3 ppm. FTIR (solid, ATR) ν_{max} /cm^{-1}: 3196 (NH), 3053 (br., OH), 2918, 2820, 1578, 1560, 1443, 1412, 1366, 1182, 1161, 1130, 1120, 1099, 1082, 1007, 984, 881, 792, 745, 658, 637, 617. UV–Vis (MeOH): λ_{max} /nm (ε / Lmol^{-1} cm^{-1}): 242 (7400), 298 (8960). HRMS (ES+) found *m/z* 283.1560 $[M + H]^+$, calculated *m/z* 283.1559 for $[C_{16}H_{19}N_4O]$.

2.2. Synthesis of 6-morpholino-5,6-dihydro-1,10-phenanthrolin-5-ol (2)

Same procedure as **1**, but using 5,6-epoxy-5,6-dihydro-1,10-phenanthroline (0.750 g, 3.9 mmol) and morpholine (0.33 mL, 11.7 mmol). The resultant brown resin-like residue was purified by DCM/hexane anti-solvent recrystallisation, the precipitate was retrieved through filtration and washed with hexane (3 × 10 mL) to yield the product as a cream powder (1.090 g, 100 %). ^{1}H NMR (300 MHz, $(CD_3)_2SO$, 298 K) δ_H: 8.61 (2H, app. d, J_{HH} = 4.4 Hz), 8.01–7.91 (2H, m), 7.42 (2H, app. dd, J_{HH} = 4.5, 3.1 Hz), 5.81 (1H, d, J_{HH} = 5.8 Hz), 5.06–5.01 (1H, O*H*, m), 3.86 (1H, d, J_{HH} = 7.9 Hz), 3.53 (4H, t, J_{HH} = 4.6 Hz), 2.81–2.69 (2H, m), 2.61–2.43 (2H, m) ppm. $^{13}C\{^{1}H\}$ NMR (101 MHz, $(CD_3)_2SO$, 298 K) δ_C: 151.2, 149.8, 148.9, 148.7, 136.8, 136.5, 134.8, 132.1, 124.1, 123.9, 67.6, 66.9, 66.8, 50.0 ppm. FTIR (solid, ATR) ν_{max} /cm^{-1}: 3240, 3051, 2951, 2845, 1578, 1560, 1450, 1427, 1414, 1152, 1113, 1069, 1005, 926, 881, 851, 799, 746, 708, 636, 546. UV–Vis (MeOH): λ_{max} /nm (ε/Lmol^{-1} cm^{-1}): 243 (7360), 297 (9110). HRMS (ES+) found *m/z* 284.1398 $[M + H]^+$, calculated *m/z* 284.1399 for $[C_{16}H_{18}N_3O_2]$.

2.3. Synthesis of 6-(4-methylpiperazin-1-yl)-5,6-dihydro-1,10-phenanthrolin-5-ol. (3)

Same procedure as **1**, but using 5,6-epoxy-5,6-dihydro-1,10-phenanthroline (0.250 g, 1.3 mmol) and 4-methyl-piperazine (0.43 mL, 3.9 mmol). The resultant brown resin-like residue was purified by DCM/hexane antisolvent recrystallisation, the precipitate was retrieved through filtration and washed with hexane (3 × 10 mL) to yield the product as a cream powder (0.321 g, 79 %). ^{1}H NMR (300 MHz, $(CD_3)_2SO$, 298 K) δ_H: 8.61 (2H, app. td, J_{HH} = 5.1, 1.7 Hz), 7.95 (1H, dd, J_{HH} = 7.7, 0.8 Hz), 7.92 (1H, dd, J_{HH} = 7.7, 0.8 Hz), 7.42 (2H, app. Ddd, J_{HH} = 7.7, 4.8, 3.8 Hz), 5.10 (1H, d, J_{HH} = 8.0 Hz), 3.97 (1H, d, J_{HH} = 8.0 Hz), 2.88 (2H, br. s), 2.65 (2H, br. dt, J_{HH} = 10.7, 4.6 Hz), 2.44 (4H, br. s), 2.25 (3H, s) ppm. ^{13}C{^{1}H} NMR (101 MHz, $(CD_3)_2SO$, 298 K): δ_C: 151.1, 148.8, 148.6, 136.7, 134.7, 132.4, 124.0, 123.9, 67.6, 66.5, 55.4, 45.9 ppm. FTIR (solid, ATR) ν_{max} /cm^{-1}: 3186, 3055, 2934, 2797, 1578, 1560, 1456, 1416, 1369, 1348, 1280, 1140, 1069, 1007, 800, 745, 546, 436. UV–Vis (MeOH): λ_{max} /nm (ε/Lmol^{-1} cm^{-1}): 242 (6970), 297 (8510). HRMS (ES+) found *m/z* 297.1722 [M + H]$^{+}$, calculated *m/z* 297.1715 for $[C_{17}H_{21}N_4O]$.

2.4. Synthesis of 6-(4-methylpiperidin-1-yl)-5,6-dihydro-1,10-phenanthrolin-5-ol. (4)

Same procedure as **1**, but using 5,6-epoxy-5,6-dihydro-1,10-phenanthroline (0.200 g, 1.0 mmol) and 4-(trifluoromethyl)piperidine (0.48 mL, 4.1 mmol). The product was precipitated out by anti-solvent recrystallisation, using dichloromethane (1 × 20 mL) and hexane (2 × 20 mL) and filtered to yield a cream powder (0.271 g, 90 %). ^{1}H NMR (500 MHz, $CDCl_3$, 298 K) δ_H: 8.64 (1H, dd, J_{HH} = 4.7, 1.5 Hz), 8.63 (1H, dd, J_{HH} = 4.7, 1.5 Hz), 7.92 (1H, ddd, J_{HH} = 7.6, 1.2, 0.9 Hz), 7.90 (1H, ddd, J_{HH} = 7.7, 1.1, 1.0 Hz), 7.13 (1H, dd, J_{HH} = 8.0, 4.7 Hz), 7.13 (1H, dd, J_{HH} = 8.0, 4.7 Hz), 4.94 (1H, d,J_{HH} = 10 Hz), 3.85 (1H, d,J_{HH} = 9.9 Hz), 2.76 (2H, td, J_{HH} = 11.5, 2.3 Hz), 2.66 (1H, dt, J_{HH} = 11.3, 3.1 Hz), 2.51 (1H, td, J_{HH} = 11.3, 2.4 Hz), 1.48 (2H, dt, J_{HH} = 12.4, 3.4 Hz), 1.25 (1H, m), 1.06 (2H, td, J_{HH} = 12.4, 3.1 Hz), 0.79 (3H, d,J_{HH} = 6.5 Hz) ppm. ^{13}C{^{1}H} NMR (500 MHz, $CDCl_3$, 298 K) δ_C: 151.3, 149.6, 149.5, 149.3, 136.1, 135.6, 133.8, 132.5, 124.2, 123.9, 68.5, 68.2, 50.6, 49.6, 35.6, 35.3, 31.2, 22.1 ppm. FTIR (solid, ATR) ν_{max} /cm^{-1}: 3246 (br. OH), 2908, 2868, 2208, 1580, 1562, 1416, 1323, 1240, 1180, 1080, 976, 907, 799, 723, 640. UV–Vis (MeOH): λ_{max} /nm (ε/Lmol^{-1} cm^{-1}): 202 (41050), 243 (10450), 300 (11780). HRMS (ES+): found *m/z* 296.1773 [M + H]$^{+}$, calculated *m/z* 296.1685 for $[C_{18}H_{22}N_3O]$.

2.5. Synthesis of 6-(4-trifluoromethylpiperidin-1-yl)-5,6-dihydro-1,10-phenanthrolin-5-ol (5)

Same procedure as **1**, but using 5,6-epoxy-5,6-dihydro-1,10-phenanthroline (0.200 g, 1.0 mmol) and 4-(trifluoromethyl)piperidine (0.55 mL, 4.1 mmol). The product was precipitated from dichloromethane and hexane and filtered to yield a white powder (0.193 g, 54 %). ^{1}H NMR (500 MHz, $CDCl_3$, 298 K) δ_H: 8.63 (2H, ddd, J_{HH} = 6.8, 4.7, 1.7 Hz), 7.97–7.89 (2H, m), 7.29 (2H, ddd, J_{HH} = 14.9, 7.7, 4.7 Hz), 5.14 (1H, d, J_{HH} = 9.8 Hz), 4.05 (1H, d, J_{HH} = 9.8 Hz), 3.07–2.94 (2H, m), 2.88 (2H, dt, J_{HH} = 11.8, 3.8 Hz), 2.57 (1H, td, J_{HH} = 11.7, 2.5 Hz), 2.07–1.94 (1H, m, C*H*CF$_3$), 1.89–1.81 (2H, m), 1.67–1.52 (2H, m) ppm ^{13}C{^{1}H} NMR (500 MHz, CD_3OD, 298 K) δ_C: 151.9, 150.7, 150.1, 149.9, 138.5, 137.9, 136.3, 134.0, 128.0, 125.8–125.7 (m), 69.6, 68.8, 53.0, 49.5, 46.9, 26.9, 26.3 ppm. ^{19}F{^{1}H} NMR (400 MHz, CD_3OD, 298 K) δ_F: −75.38 ppm. FTIR (solid, ATR) ν_{max} /cm^{-1}: 3253 (br. OH), 2955, 2862, 2342, 1582, 1564, 1418, 1341, 1252, 1125, 1078, 1003, 802, 745, 629. UV–Vis (MeOH): λ_{max} /nm (ε/Lmol^{-1} cm^{-1}): 203 (33720), 241 (11130), 298 (12010). HRMS (ES+) found *m/z* 350.1476 [M + H]$^{+}$, calculated *m/z* 350.1401 for $[C_{18}H_{19}F_3N_3O]$.

2.6. Synthesis of 6-(4-phenylpiperazin-1-yl)-5,6-dihydro-1,10-phenanthrolin-5-ol (6)

Same procedure as **1**, but using 5,6-epoxy-5,6-dihydro-1,10-phenanthroline (0.200 g, 1.0 mmol), and 1-phenylpiperazine (0.62 mL, 4.1 mmol). The mixture was heated to reflux under nitrogen for 45 h. The reaction was cooled at room temperature and the solvent was removed in vacuo to give a light orange oil. The product was precipitated from dichloromethane and hexane and filtered to yield a white powder (0.126 g, 34 %). ^{1}H NMR (500 MHz, $CDCl_3$, 298 K) δ_H: 8.68 (1H, dd, J_{HH} = 4.5, 1.3 Hz), 8.66 (1H, dd, J_{HH} = 4.9, 1.5 Hz), 7.98 (1H, ddd, J_{HH} = 7.7, 1.6, 0.9 Hz), 7.92 (1H, ddd, J_{HH} = 7.7, 1.5, 0.7 Hz), 7.30 (1H, dd, J_{HH} = 7.5, 4.7 Hz), 7.27 (1H, dd, J_{HH} = 6.0, 4.4 Hz), 7.25 (2H, dd, J_{HH} = 7.1, 1.4 Hz), 6.90 (2H, dd, J_{HH} = 8.7, 0.9 Hz), 6.87 (1H, tt, J_{HH} = 7.2, 1.0 Hz), 5.17 (1H, d,J_{HH} = 9 Hz), 4.09 (1H, d,J_{HH} = 9.1 Hz), 3.16 (4H, t, J_{HH} = 4.9 Hz), 3.04 (2H, td, J_{HH} = 8.4, 4.7 Hz), 2.88 (2H, td, J_{HH} = 8.4, 4.8 Hz) ppm. ^{13}C{^{1}H} NMR (500 MHz, $CDCl_3$, 298 K) δ_C: 151.4, 151.2, 149.7, 149.6, 149.5, 136.7, 135.6, 134.5, 132.0, 129.5, 129.3, 124.3, 124.2, 120.2, 117.2, 116.5, 68.6, 67.5, 50.4, 49.6, 47.0, 43.4 ppm. FTIR (solid, ATR) ν_{max} /cm^{-1}: 3296 (br. OH), 2938, 2822, 2183, 1599, 1580, 1497, 1418, 1310, 1231, 1146, 1070, 1007, 920, 800, 745, 691. UV–Vis (MeOH): λ_{max} /nm (ε/Lmol^{-1} cm^{-1}): 203 (57240), 247 (21240), 301 (11070). HRMS (ES+) found *m/z* 359.1872 [M + H]$^{+}$, calculated *m/z* 359.1794 for $[C_{22}H_{23}N_4O]$.

2.7. Synthesis of 6-(4-benzhydrylpiperazin-1-yl)-5,6-dihydro-1,10-phenanthrolin-5-ol. (7)

Same procedure as **1**, but using 5,6-epoxy-5,6-dihydro-1,10-phenanthroline (0.200 g, 1.0 mmol), and 1-benzhydrylpiperazine (1.029 g, 4.1 mmol). The mixture was heated to reflux under nitrogen for 54 h. The product was precipitated using chloroform and hexane (3 × 20 mL) and filtered to yield white powder (0.125 g, 27 %). ^{1}H NMR (500 MHz, $CDCl_3$, 298 K) δ_H: 8.69 (1H, dd, J_{HH} = 4.7, 1.8 Hz), 8.68 (1H, dd, J_{HH} = 4.7, 1.9 Hz), 7.92 (1H, ddd, J_{HH} = 7.9, 1.5, 0.9 Hz), 7.90 (1H, ddd, J_{HH} = 7.8, 1.5, 0.8 Hz), 7.42 (4H, dd, J_{HH} = 7.6, 2.9 Hz), 7.29 (1H, dd, J_{HH} = 7.1, 4.7 Hz), 7.27 (1H, dd, J_{HH} = 8.4, 4.8 Hz), 7.26 (4H, td, J_{HH} = 7.7, 1.3 Hz), 7.18 (2H, tt, J_{HH} = 7.4, 1.2 Hz), 5.07 (1H, d,J_{HH} = 9.0 Hz), 4.26 (1H, s), 4.00 (1H, d,J_{HH} = 8.9 Hz), 2.91 (2H, t,J_{HH} = 5.2), 2.81 (2H, t, J_{HH} = 5.0 Hz), 2.45 (4H, br s) ppm. ^{13}C{^{1}H} NMR (500 MHz, $CDCl_3$, 298 K) δ_C: 151.4, 150.0, 149.8, 149.7, 142.6, 142.5, 136.5, 135.1, 134.2, 131.6, 128.6, 128.9, 128.0, 127.1, 124.3, 123.9, 76.4, 68.7, 67.5, 52.9, 49.6 ppm. FTIR (solid, ATR) ν_{max} /cm^{-1}: 3294 (br. OH), 3059, 2808, 2151, 1580, 1560, 1418, 1279, 1136, 1005, 800, 745, 704. UV–Vis (MeOH): λ_{max} /nm (ε/Lmol^{-1} cm^{-1}): 203 (70440), 253 (10930), 302 (11240). HRMS (ES+): found *m/z* 449.2335 [M + H]$^{+}$, calculated *m/z* 449.2263 for $[C_{29}H_{29}N_4O]$.

2.8. Synthesis of 5-(piperazin-1-yl)-1,10-phenthanthroline (L^1)

NaH (0.150 g, 3.8 mmol, 60 % dispersion in oil) was carefully added portion-wise to a suspension of **1** (0.770 g, 2.7 mmol) in dry THF (24 mL) and heated to reflux for 16 h under nitrogen where a colour change to a dark orange colour was observed. The excess NaH was quenched by carefully adding MeOH (6 mL) to the reaction mixture. The reaction was cooled to room temperature and the solvent was removed under vacuum. The residue was dissolved in EtOH and filtered, the filtrate was taken, and solvent remove under vacuum to yield the product as a sticky brown compound (0.550 g, 77 %). ^{1}H NMR (300 MHz, $(CD_3)_2SO$, 298 K) δ_H: 9.07 (1H, dd, J_{HH} = 4.2, 1.7 Hz), 8.92 (1H, dd, J_{HH} = 4.3, 1.7 Hz), 8.59 (1H, dd, J_{HH} = 8.4, 1.8 Hz), 8.37 (1H, dd, J_{HH} = 8.2, 1.7 Hz), 7.77 (1H, dd, J_{HH} = 8.3, 4.2 Hz), 7.68 (1H, dd, J_{HH} = 8.1, 4.3 Hz), 7.45 (1H, s), 3.01 (8H, overlapping s), 2.58 (1H, s, N*H*) ppm. ^{13}C{^{1}H} NMR (101 MHz, $(CD_3)_2SO$, 298 K): δ_C: 149.7, 148.2, 147.9, 146.4, 143.1, 135.4, 132.5, 128.9, 125.3, 123.5, 122.9, 112.7, 54.1, 45.9 ppm. FTIR (solid, ATR) ν_{max} /cm^{-1}: 3271, 2920, 2849, 1609, 1587, 1557, 1510, 1467,

1454, 1422, 1404, 1371, 1290, 1278, 1215, 1150, 1121, 1011, 997, 910, 864, 827, 804, 743. UV–Vis (MeCN): λ_{max} /nm (ε/Lmol^{-1} cm^{-1}): 201 (27540), 228 (31850), 278 (20780), 321 (3960). HRMS (ES+) found *m/z* 265.1454 [M + H]$^+$, calculated *m/z* 265.1453 for [$C_{16}H_{17}N_4$].

2.9. Synthesis of 4-morpholine-1,10-phenanthroline (L^2)

Same procedure as **L^1**, but using NaH (0.120 g, 3.4 mmol, 60 % dispersion in oil), **2** (0.800 g, 2.8 mmol) and dry THF (25 mL). A cream powder was isolated (0.693 g, 93 %). ^{1}H NMR (400 MHz, $(CD_3)_2SO$, 298 K) δ_H: 9.06 (1H, dd, J_{HH} = 4.2, 1.4 Hz), 8.94 (1H, dd, J_{HH} = 4.3, 1.4 Hz), 8.59 (1H, dd, J_{HH} = 8.3, 1.5 Hz), 8.36 (1H, dd, J_{HH} = 8.3, 1.6 Hz), 7.76 (1H, dd, J_{HH} = 8.3, 4.3 Hz), 7.68 (1H, dd, J_{HH} = 8.0, 4.2 Hz), 7.48 (1H, s), 3.90 (4H, t,J_{HH} = 4.4 Hz), 3.09 (4H, app. s) ppm. ^{13}C{^{1}H} NMR (101 MHz, $(CD_3)_2SO$, 298 K): δ_C: 149.9, 148.5, 147.1, 146.4, 143.2, 135.6, 132.5, 128.8, 125.1, 123.6, 123.0, 113.0, 66.4, 53.1 ppm. FTIR (solid, ATR) ν_{max} /cm^{-1}: 3424, 1955, 2853, 1607, 1589, 1564, 1450, 1422, 1373, 1260, 1209, 1109, 1013, 924, 908, 862, 841, 808, 799, 745, 689, 625. UV–Vis (MeCN): λ_{max} /nm (ε/Lmol^{-1} cm^{-1}): 201 (32240), 228 (38180), 278 (19470), 321 (4799). HRMS (AP+) found *m/z* 266.1296 [M + H]$^+$, calculated *m/z* 266.1293 for [$C_{16}H_{16}N_3O$].

2.10. Synthesis of 5-(4-methylpiperazin-1-yl)-1,10-phenanthroline (L^3)

Same procedure as **L^1**, but using NaH (0.160 g, 0.8 mmol, 60 %), **3** (0.100 g, 0.7 mmol) and dry THF (15 mL). The product was isolated as a sticky orange-brown compound (0.092 g, 98 %). ^{1}H NMR (300 MHz, $(CD_3)_2SO$, 298 K) δ_H: 9.06 (1H, dd, J_{HH} = 4.2, 1.4 Hz), 8.92 (1H, dd, J_{HH} = 4.2, 1.5 Hz), 8.55 (1H, dd, J_{HH} = 8.3, 1.4 Hz), 8.37 (1H, dd, J_{HH} = 8.1, 1.3 Hz), 7.78 (1H, dd, J_{HH} = 8.3, 4.3 Hz), 7.68 (1H, dd, J_{HH} = 8.1, 4.3 Hz), 7.47 (1H, s), 3.09 (4H, app. s), 2.62 (4H, br. t,J_{HH} = 4.3 Hz), 2.29 (3H, s) ppm. ^{13}C{^{1}H} NMR (101 MHz, $(CD_3)_2SO$, 298 K): δ_C: 149.7, 148.3, 147.2, 146.5, 143.3, 135.4, 132.3, 128.8, 125.3, 123.5, 122.9, 112.9, 54.9, 52.5, 45.8 ppm. FTIR (solid, ATR) ν_{max} /cm^{-1}: 3300, 2941, 2803, 1608, 1568, 1508, 1483, 1452, 1422, 1369, 1285, 1215, 1138, 1076, 1007, 868, 829, 793, 745. UV–Vis (MeCN): λ_{max} /nm (ε/Lmol^{-1} cm^{-1}): 202 (32900), 228 (35790), 279 (18240), 321 (4840). HRMS (ES+) found *m/z* 279.1609 [M + H]$^+$, calculated *m/z* 279.1610 for [$C_{17}H_{19}N_4$].

2.11. Synthesis of 5-(4-methylpiperidin-1-yl)-1,10-phenanthroline (L^4)

Same procedure as **L^1**, but using NaH (0.029 g, 1.0 mmol), **4** (0.169 g, 0.5 mmol) and dry THF (25 mL). The product was isolated as a brown oil (0.037 g, 22 %). ^{1}H NMR (500 MHz, $CDCl_3$, 298 K) δ_H: 9.13 (1H, dd, J_{HH} = 4.3, 1.7 Hz), 9.00 (1H, dd, J_{HH} = 4.4, 1.7 Hz), 8.52 (1H, dd, J_{HH} = 8.3, 1.8 Hz), 8.07 (1H, dd, J_{HH} = 8.1, 1.7 Hz), 7.59 (1H, dd, J_{HH} = 8.3, 4.3 Hz), 7.50 (1H, dd, J_{HH} = 8.1, 4.3 Hz), 7.17 (1H, s), 3.43–3.35 (2H, m), 2.77 (2H, app. t, J_{HH} = 11.6 Hz), 1.86–1.78 (2H, m), 1.66–1.50 (3H, m), 1.05 (3H, d, J_{HH} = 5.9 Hz) ppm. ^{13}C{^{1}H} NMR (500 MHz, CD_3OD, 298 K) δ_C: 150.0, 148.8, 148.4, 147.2, 143.9, 135.0, 132.7, 129.2, 126.3, 123.2, 122.4, 112.5, 53.9, 34.7, 31.0, 22.0 ppm. FTIR (solid, ATR) ν_{max} /cm^{-1}: 2920, 2841, 1607, 1587, 1506, 1452, 1420, 1377, 1211, 1072, 978, 745. UV–Vis (MeCN): λ_{max} /nm (ε/Lmol^{-1} cm^{-1}): 229 (48730), 279 (19310), 323 (6210). HRMS (ES+): found *m/z* 278.1666 [M + H]$^+$, calculated *m/z* 278.1579 for [$C_{18}H_{20}N_3$].

2.12. Synthesis of 5-(4-trifluoromethylpiperidin-1-yl)-1,10-phenanthroline (L^5)

Same procedure as **L^1**, but using NaH (0.021 g, 0.9 mmol), **5** (0.150 g, 0.4 mmol) and dry THF (25 mL). The product was isolated as a brown solid (0.093 g, 66 %). ^{1}H NMR (300 MHz, $CDCl_3$, 298 K) δ_H: 9.18 (1H, dd, J_{HH} = 4.3, 1.8 Hz), 9.07 (1H, dd, J_{HH} = 4.3, 1.7 Hz), 8.53 (1H, dd, J_{HH} = 8.3, 1.8 Hz), 8.13 (1H, dd, J_{HH} = 8.1, 1.7 Hz), 7.65 (1H, dd, J_{HH} = 8.3, 4.3 Hz), 7.57 (1H, dd, J_{HH} = 8.0, 4.3 Hz), 7.25 (1H, s), 3.56 (2H, app. d, J_{HH} = 11.6 Hz), 2.84 (2H, td, J_{HH} = 12.1, 2.4 Hz), 2.35–2.22 (1H, m, C*H*CF$_3$), 2.14–2.06 (2H, m), 2.06–1.93 (2H, m) ppm. ^{13}C{^{1}H} NMR (125 MHz, $CDCl_3$, 298 K) δ_C: 150.3, 149.0, 147.9, 147.3, 144.3, 135.2, 132.3, 128.9, 128.6, 126.1, 123.4, 122.7, 113.3, 52.5, 25.4 ppm. ^{19}F {^{1}H} NMR (470 MHz, CD_3OD, 298 K) δ_F: −75.2 ppm. FTIR (solid, ATR) ν_{max} /cm^{-1}: 2924, 2818, 2357, 1611, 1587, 1450, 1422, 1383, 1327, 1250, 1134, 1077, 1003, 897, 745. UV–Vis (MeCN): λ_{max} /nm (ε/Lmol^{-1} cm^{-1}): 229 (45740), 277 (20330), 316 (6160). HRMS (ES+) found *m/z* 332.1375 [M + H]$^+$, calculated *m/z* 332.1296 for [$C_{18}H_{17}F_3N_3$].

2.13. Synthesis of 5-(4-phenylpiperazin-1-yl)-1,10-phenanthroline (L^6)

Same procedure as **L^1**, but using NaH (0.012 g, 0.5 mmol), **6** (0.090 g, 0.3 mmol) and dry THF (25 mL). The product was isolated as a light brown powder (0.058 g, 68 %). ^{1}H NMR (500 MHz, $CDCl_3$, 298 K) δ_H: 9.20 (1H, dd, J_{HH} = 4.3, 1.7 Hz), 9.08 (1H, dd, J_{HH} = 4.3, 1.7 Hz), 8.64 (1H, dd J_{HH} = 8.3, 1.8 Hz), 8.16 (1H, dd, J_{HH} = 8.1, 1.7 Hz), 7.66 (1H, dd, J_{HH} = 8.3, 4.3 Hz), 7.59 (1H, dd, J_{HH} = 8.0, 4.3 Hz), 7.37–7.30 (3H, m), 7.08–7.03 (2H, m), 6.96–6.90 (1H, m), 3.51 (4H, s), 3.35 (4H, s) ppm. ^{13}C{^{1}H} NMR (500 MHz, $CDCl_3$, 298 K) δ_C: 151.2, 150.2, 148.9, 147.5, 147.3, 144.3, 135.1, 132.3, 129.3, 128.9, 125.8, 123.3, 122.5, 120.2, 116.3, 113.0, 53.0, 49.7 ppm. FTIR (solid, ATR) ν_{max} /cm^{-1}: 2926, 2824, 2193, 1611, 1597, 1505, 1449, 1379, 1233, 1013, 928, 741. UV–Vis (MeCN): λ_{max} /nm (ε/Lmol^{-1} cm^{-1}): 229 (43830), 246 (22650), 277 (20250), 316 (5690). HRMS (ES+): found *m/z* 341.1769 [M + H$^+$], calculated *m/z* 340.1688 for [$C_{22}H_{20}N_4$].

2.14. Synthesis of 5-(4-benzhydrylpiperazin-1-yl)-1,10-phenanthroline (L^7)

Same procedure as **L^1**, but using NaH (0.026 g, 0.4 mmol), **7** (0.090 g, 0.2 mmol) and dry THF (25 mL). The product was retrieved as a light brown powder (0.082 g, 87 %). ^{1}H NMR (500 MHz, $CDCl_3$, 298 K) δ_H: 9.14 (1H, dd, J_{HH} = 4.3, 1.7 Hz), 9.04 (1H, dd, J_{HH} = 4.3, 1.7 Hz), 8.53 (1H, dd, J_{HH} = 8.3, 1.8 Hz), 8.11 (1H, dd, J_{HH} = 8.1, 1.7 Hz), 7.59–7.52 (2H, m), 7.52–7.46 (4H, m), 7.34–7.29 (4H, m), 7.25 (1H, s), 7.24–7.19 (2H, m), 4.41 (1H, s), 3.21 (4H, s), 2.73 (4H, s) ppm. ^{13}C{^{1}H} NMR (500 MHz, CD_3OD, 298 K) δ_C: 149.6, 148.2, 147.4, 146.8, 143.7, 142.5, 134.9, 132.2, 128.3, 127.6, 126.8, 125.6, 122.9, 122.1, 116.4, 112.4, 75.9, 52.8, 51.9 ppm. FTIR (solid, ATR) ν_{max} /cm^{-1}: 2947, 2814, 2168, 1609, 1558, 1449, 1420, 1379, 1215, 1007, 964, 872, 702, 621. UV–Vis (MeCN): λ_{max} /nm (ε/Lmol^{-1} cm^{-1}): 229 (39550), 278 (13720), 319 (4310). HRMS (ES+): found *m/z* 431.2237 [M + H$^+$], calculated *m/z* 430.2157 for [$C_{22}H_{20}N_4$].

2.15. Synthesis of cholesteryl carbamate-5-(piperazin-1-yl)-1,10-phenanthroline (L^8)

L^1 (0.200 g, 0.8 mmol) and cholesteryl chloroformate (0.340 g, 0.8 mmol) were dissolved in dichloromethane (30 mL). The mixture was heated to reflux for 16 h. Once the reaction was cool, the solvent was removed under vacuum to yield a crystalline mustard yellow product. (0.414 g, 81 %). ^{1}H NMR (300 MHz, $CDCl_3$, 298 K) δ_H: 9.38 (2H, dd, J_{HH} = 12.5, 3.8 Hz), 8.69 (1H, dd, J_{HH} = 8.4, 1.5 Hz), 8.44 (1H, d, J_{HH} = 7.8 Hz), 7.83 (2H, dd, J_{HH} = 8.2, 4.5 Hz), 7.35 (1H, s), 5.41 (1H, s), 4.58 (1H, m) 3.77 (4H, s), 3.18 (4H, s), 1.01 (3H, s), 0.90 (3H, d,J_{HH} = 3.6 Hz), 0.86 (3H, d,J_{HH} = 2.0 Hz), 0.67 (3H, s) ppm.^{13}C{^{1}H} NMR (101 MHz, $CDCl_3$, 298 K): δ_C: 155.3, 140.9, 139.5, 123.1, 121.8, 78.0, 71.9, 56.8, 56.3, 56.2, 54.6, 50.3, 50.1, 43.4, 39.1, 38.2, 37.4, 36.7, 36.3, 35.9, 32.0, 28.8, 28.4, 27.8, 24.4, 23.0, 21.2, 19.5, 18.8, 12.0 ppm. FTIR (solid, ATR) ν_{max} /cm^{-1}: 3356, 2932, 2866, 1692, 1593, 1460, 1423, 1377, 1333, 1285, 1240, 1221, 1119, 1063, 1011, 766, 746, 746, 729, 596, 444, 419, 410. UV–Vis ($CHCl_3$): λ_{max} /nm (ε/Lmol^{-1} cm^{-1}): 298 (5700), 341 (1900). HRMS (ES+) found *m/z* 677.4800 [M + H$^+$], calculated *m/z* 677.4785 for [$C_{44}H_{61}N_4O_2$].

2.16. Synthesis of $[Ru(bipy)_2(L^1)](PF_6)_2$

$[Ru(bipy)_2Cl_2]$ (0.107 g, 0.2 mmol), **L^1** (0.059 g, 0.2 mmol) and $NaPF_6$ (0.082 g, 0.5 mmol) were combined in EtOH (10 mL). The mixture was degassed with N_2 for 20 min and heated to reflux for 120 h. The reaction was partially cooled and 0.1 M NH_4PF_6 solution (20 mL) was added. The precipitate was retrieved through filtration and washed with distilled water (3 × 10 mL). The product was extracted from the filtrate into DCM/MeCN (3:1) and washed with distilled water (3 × 10 mL) and brine (1 × 10 mL). The organic layer was then dried with anhydrous $Mg(SO_4)$ and filtered. The solvent was then removed under vacuum to yield the product as a bright red powder. (0.104 g, 69 %). ^{1}H NMR (500 MHz, CD_3CN, 298 K) δ_H: 8.71 (1H, dd, J_{HH} = 8.5, 1.3 Hz), 8.55–8.52 (2H, m), 8.51–8.43 (3H, m), 8.10 (2H, ddd, J_{HH} = 7.9, 2.9, 1.6 Hz), 8.09–8.05 (1H, m), 8.00 (2H, app. td J_{HH} = 7.9, 1.5 Hz), 7.95 (1H, dd, J_{HH} = 5.2, 1.2 Hz), 7.88–7.80 (2H, m), 7.76 (1H, s), 7.72 (1H, dd, J_{HH} = 8.4, 5.2 Hz), 7.66 (1H, dd, J_{HH} = 8.3, 5.2 Hz), 7.57–7.52 (2H, m), 7.44 (2H, app. Tdt, J_{HH} = 6.3, 2.9, 1.4 Hz), 7.26–7.19 (2H, m), 3.65–3.33 (8H, m). $^{13}C\{^1H\}$ NMR (101 MHz, CD_3CN, 298 K): δ_C: 158.26, 158.25, 158.0, 153.4, 153.0, 152.94, 152.91, 152.86, 151.9, 149.7, 149.3, 146.4, 138.8, 138.72, 138.70, 136.8, 134.4, 132.1, 129.2, 128.53, 128.45, 128.4, 127.2, 126.6, 125.25, 125.23, 125.16, 116.0, 50.9, 45.5 ppm. FTIR (solid, ATR) ν_{max} /cm^{-1}: 3248, 2953, 2928, 2843, 2605, 1516, 1465, 1447, 1423, 1267, 1123, 1015, 997, 826, 804, 760, 741, 729, 556, 523, 509. UV–Vis (CH_3CN): λ_{max} /nm (ε/$Lmol^{-1}$ cm^{-1}): 225 (16760), 245 (18010), 255 (16100), 285 (28690), 334 (3990), 429 (5120), 452 (5970). HRMS (ES+) found *m/z* 339.0900, calculated *m/z* 339.0901 for $[C_{36}H_{32}N_8Ru]^{2+}$.

2.17. Synthesis of $[Ru(bipy)_2(L^2)](PF_6)_2$

Same procedure as **$[Ru(bipy)_2(L^1)](PF_6)_2$**, but using $[Ru(bipy)_2Cl_2]$ (0.050 g, 0.1 mmol) and **L^2** (0.027 g, 0.1 mmol). Product isolated as a dark orange powder (0.067 g, 96 %). ^{1}H NMR (500 MHz, CD_3CN, 298 K) δ_H: 8.75 (1H, dd, J_{HH} = 8.5, 1.3 Hz), 8.55–8.51 (2H, m), 8.49 (2H, dd, J_{HH} = 8.2, 1.9 Hz), 8.44 (1H, dd, J_{HH} = 8.3, 1.2 Hz), 8.09 (2H, tdd, J_{HH} = 8.0, 2.9, 1.5 Hz), 8.05 (1H, dd, J_{HH} = 5.2, 1.3 Hz), 8.02–7.96 (2H, m), 7.91 (1H, dd, J_{HH} = 5.2, 1.2 Hz), 7.85–7.80 (2H, m), 7.69 (1H, dd, J_{HH} = 8.5, 5.2 Hz), 7.67 (1H, s), 7.63 (1H, dd, J_{HH} = 8.3, 5.2 Hz), 7.58–7.53 (2H, m), 7.46–7.42 (2H, m), 7.24 (2H, dtd, J_{HH} = 7.1, 5.6, 1.3 Hz), 3.96 (4H, q, J_{HH} = 4.1 Hz), 3.23 (4H, d, J_{HH} = 4.9 Hz) ppm. $^{13}C\{^1H\}$ NMR (101 MHz, CD_3CN, 298 K): δ_C: 158.2, 158.2, 157.9, 153.1, 152.9, 152.9, 152.8, 151.3, 150.5, 149.7, 146.0, 138.7, 138.6, 138.6, 128.5, 128.5, 128.4, 125.2, 125.1, 125.1, 114.6, 67.5, 54.3 ppm. FTIR (solid, ATR) ν_{max} /cm^{-1}: 1620, 1603, 1466, 1447, 1422, 1258, 1117, 1070, 887, 833, 802, 760, 729, 555. UV–Vis (CH_3CN): λ_{max} /nm (ε/$Lmol^{-1}$ cm^{-1}): 225 (27260), 246 (32070), 286 (52340), 340 (8270), 429 (10420), 452 (12270). HRMS (ES+) found *m/z* 339.5825, calculated *m/z* 339.5822 for $[C_{36}H_{29}N_7ORu]^{2+}$.

2.18. Synthesis of $[Ru(bipy)_2(L^3)](PF_6)_2$

Same procedure as **$[Ru(bipy)_2(L^1)](PF_6)_2$**, but using $[Ru(bipy)_2Cl_2]$ (0.07 g, 0.1 mmol), **L^3** (0.040 g, 0.1 mmol) and $NaPF_6$ (0.053 g, 0.3 mmol). The product was isolated as a red-orange powder (0.095 g, 95 %). ^{1}H NMR (500 MHz, CD_3CN, 298 K) δ_H: 8.69 (1H, d, J_{HH} = 8.5 Hz), 8.56–8.50 (2H, m), 8.51–8.46 (3H, m), 8.12–8.07 (3H, m), 8.01 (2H, d, J_{HH} = 1.2 Hz), 7.96 (1H, dd, J_{HH} = 5.1, 0.8 Hz), 7.86–7.81 (2H, m), 7.78 (1H, s), 7.73 (1H, dd, J_{HH} = 8.4, 5.2 Hz), 7.67 (1H, dd, J_{HH} = 8.2, 5.3 Hz), 7.55 (2H, d, J_{HH} = 5.4 Hz), 7.48–7.42 (2H, m), 7.24 (2H, td, J_{HH} = 5.9, 1.4 Hz, 1H), 3.55 (4H, s), 3.51–3.40 (4H, m), 2.97 (3H, s) ppm. $^{13}C\{^1H\}$ NMR (101 MHz, CD_3CN, 298 K): δ_C: 158.3, 158.2, 158.0, 153.5, 153.0, 152.9, 152.9, 152.9, 152.1, 149.7, 148.6, 146.5, 138.8, 138.7, 138.7, 136.8, 134.2, 132.0, 129.2, 128.6, 128.5, 128.5, 128.4, 127.3, 126.7, 125.3, 125.2, 125.2, 116.3, 55.1, 50.9, 44.3 ppm. FTIR (solid, ATR) ν_{max} /cm^{-1}: 2928, 2843, 1626, 1603, 1466, 1447, 1425, 1260, 1233, 1211, 986, 827, 764, 743, 733, 557. UV–Vis (MeCN): λ_{max} /nm (ε/$Lmol^{-1}$ cm^{-1}): 227 (35080), 244 (38140), 255 (32330), 286 (59990), 339 (11960), 429 (14110), 451 (15790). HRMS (ES+) found *m/z* 346.0976, calculated *m/z* 346.0980 for $[C_{37}H_{32}N_8Ru]^{2+}$.

2.19. Synthesis of $[Ru(bipy)_2(L^4)](PF_6)_2$

Same procedure as **$[Ru(bipy)_2(L^1)](PF_6)_2$**, but using $[Ru(bipy)_2Cl_2]$ (0.061 g, 0.1 mmol) and **L^4** (0.035 g, 0.1 mmol). Product isolated as an orange solid (0.116 g, 93 %). ^{1}H NMR (500 MHz, $(CD_3)_2CO$), 298 K) δ_H: 8.86–8.77 (5H, m), 8.60 (1H, dd, J_{HH} = 8.3, 1.2 Hz), 8.38 (1H, dd, J_{HH} = 5.2, 1.2 Hz), 8.24 (2H, tdd, J_{HH} = 8.0, 3.0, 1.5 Hz), 8.19 (1H, dd, J_{HH} = 5.2, 1.2 Hz), 8.17–8.11 (4H, m), 7.93–7.86 (3H, m), 7.78 (2H, d, J_{HH} = 1.1 Hz), 7.64–7.59 (2H, m), 7.43–7.36 (2H, m), 3.62–3.52 (2H, m), 2.98 (2H, dtd, J_{HH} = 31.3, 11.7, 2.4 Hz), 1.93–1.84 (2H, m), 1.71–1.57 (3H, m), 1.06 (3H, d, J_{HH} = 6.2 Hz). $^{13}C\{^1H\}$ NMR (125 MHz, $(CD_3)_2CO$), 298 K) δ_C: 158.4, 158.4, 158.2, 158.1, 153.2, 152.9, 152.9, 152.8, 152.7, 151.6, 151.0, 149.7, 145.8, 138.9, 138.8, 136.6, 134.8, 132.5, 129.7, 128.7, 128.6, 128.5, 127.2, 126.6, 125.3, 125.2, 114.4, 54.8, 54.5, 35.2, 31.5, 22.2 ppm. FTIR (solid, ATR) ν_{max} /cm^{-1}: 2922, 2853, 1622, 1597, 1456, 1423, 1387, 1128, 1080, 982, 829, 556. UV–Vis (MeCN): λ_{max} /nm (ε/$Lmol^{-1}$ cm^{-1}): 227 (28080), 246 (34600), 286 (53120), 349 (8810), 419 (9800), 453 (12540). HRMS (ES+): found *m/z* 346.6071, calculated *m/z* 346.6071 for $[C_{38}H_{35}N_7Ru]^{2+}$.

2.20. Synthesis of $[Ru(bipy)_2(L^5)](PF_6)_2$

Same procedure as **$[Ru(bipy)_2(L^1)](PF_6)_2$**, but using $[Ru(bipy)_2Cl_2]$ (0.117 g, 0.2 mmol), **L^5** (0.090 g, 0.2 mmol) and ethanol (10 mL). The product was isolated as an orange solid (0.206 g, 82 %). ^{1}H NMR (500 MHz, CD_3CN, 298 K) δ_H: 8.70 (1H, dd, J_{HH} = 8.5, 1.3 Hz), 8.55–8.50 (2H, m), 8.50–8.46 (2H, m), 8.43 (1H, dd, J_{HH} = 8.3, 1.2 Hz), 8.09 (2H, app. Dddd, J_{HH} = 8.2, 7.7, 3.5, 1.5 Hz), 8.04 (1H, dd, J_{HH} = 5.2, 1.3 Hz), 8.02–7.96 (2H, m), 7.90 (1H, dd, J_{HH} = 5.2, 1.3 Hz), 7.84 (2H, app. Dddd, J_{HH} = 8.7, 5.6, 1.5, 0.8 Hz), 7.70 (1H, dd, J_{HH} = 8.5, 5.2 Hz), 7.66 (1H, s), 7.62 (1H, dd, J_{HH} = 8.3, 5.2 Hz), 7.56 (2H, app. Dddd, J_{HH} = 5.5, 3.9, 1.5, 0.8 Hz), 7.44 (2H, app. Dddd, J_{HH} = 7.7, 5.6, 3.7, 1.3 Hz), 7.24 (2H, app. Dddd, J_{HH} = 7.7, 5.8, 4.6, 1.3 Hz), 3.72–3.54 (2H, m), 3.05–2.89 (2H, m), 2.59–2.43 (1H, m, C*H*CF_3), 2.12–2.05 (2H, m), 2.03–1.96 (2H, m) ppm.$^{13}C\{^1H\}$ NMR (125 MHz, CD_3CN, 298 K) δ_C: 158.2, 158.0, 153.2, 153.0, 152.9, 152.8, 151.3, 150.9, 149.7, 146.0, 138.8, 138.7, 136.5, 134.7, 132.4, 130,0, 129.6, 128.5, 128.4, 127.8, 127.1, 126.5, 125.2, 125.1, 114.9, 53.2, 53.0, 25.8 ppm. $^{19}F\{^1H\}$ NMR (470 MHz, CD_3CN, 298 K) δ_F: −74.3 (s), −72.9 (d [1],J_{FP} = 750 Hz) ppm. FTIR (solid, ATR) ν_{max} /cm^{-1}: 2947, 2876, 1622, 1599, 1449, 1425, 1329, 1252, 1080, 1007, 831, 760, 556. UV–Vis (MeCN): λ_{max} /nm (ε/$Lmol^{-1}$ cm^{-1}): 225 (36490), 245 (43480), 286 (69060), 340 (11150), 429 (13200), 451 (15450). HRMS (ES+): found *m/z* 373.5869, calculated *m/z* 373.5930 for $[C_{38}H_{32}F_3N_7Ru]^{2+}$.

2.21. Synthesis of $[Ru(bipy)_2(L^6)](PF_6)_2$

Same procedure as **$[Ru(bipy)_2(L^1)](PF_6)_2$**, but using $[Ru(bipy)_2Cl_2]$ (0.071 g, 0.1 mmol), **L^6** (0.050 g, 0.1 mmol) and ethanol (10 mL). The crude product was subjected to silica gel column chromatography using an eluent of $MeCN/H_2O/KNO_3$ in a 14:2:1 ratio. The product was isolated as an orange solid (0.028 g, 18 %). ^{1}H NMR (500 MHz, $(CD_3)_2CO$), 298 K) δ_H: 8.98–8.93 (1H, m), 8.82 (4H, ddd, J_{HH} = 19.6, 8.0, 3.3 Hz), 8.69–8.63 (1H, m), 8.44–8.38 (1H, m), 8.29–8.08 (7H, m), 7.91 (4H, dq, J_{HH} = 11.8, 6.2 Hz), 7.82 (1H, dd, J_{HH} = 8.3, 5.2 Hz), 7.66–7.59 (2H, m), 7.45–7.37 (2H, m), 7.29 (2H, t, J_{HH} = 7.7 Hz), 7.10 (2H, d, J_{HH} = 8.2 Hz), 6.88 (1H, t, J_{HH} = 7.3 Hz), 3.69–3.33 (m, 8H).$^{13}C\{^1H\}$ NMR (125 MHz, $(CD_3)_2CO$), 298 K) δ_C: 158.4, 158.2, 158.1, 153.3, 153.0, 152.9, 152.8, 151.4, 150.5, 149.8, 146.1, 138.9, 138.8, 138.8, 136.8, 134.8, 132.4, 130.0, 129.4, 128.7, 128.6, 127.3, 126.7, 125.3, 125.2, 117.1, 114.9, 53.9, 50.2 ppm. FTIR (solid, ATR) ν_{max} /cm^{-1}: 2828, 1622, 1599,

1447, 1423, 1227, 1161, 1020, 839, 831, 760, 556. UV–Vis (MeCN): λ_{max} /nm (ε/Lmol^{-1} cm^{-1}): 226 (35680), 247 (50010), 286 (63080), 341 (10040), 421 (11230), 452 (13560). HRMS (ES+): found *m/z* 377.1060, calculated *m/z* 377.1126 for $[C_{42}H_{36}N_8Ru]^{2+}$.

2.22. Synthesis of $[Ru(bipy)_2(L^7)](PF_6)_2$

Same procedure as **$[Ru(bipy)_2(L^1)](PF_6)_2$**, but using $[Ru(bipy)_2Cl_2]$ (0.079 g, 0.2 mmol), **L^7** (0.070 g, 0.2 mmol) and ethanol (10 mL). The product was isolated as a dark red solid (0.113 g, 14 %). ^{1}H NMR (500 MHz, $(CD_3)_2CO$), 298 K) δ_H: 8.86–8.76 (5H, m), 8.62 (1H, dd, J_{HH} = 8.3, 1.2 Hz), 8.37 (1H, dd, J_{HH} = 5.2, 1.2 Hz), 8.25–8.19 (3H, m), 8.16–8.09 (4H, m), 7.90–7.83 (4H, m), 7.80 (1H, dd, J_{HH} = 8.3, 5.2 Hz), 7.63–7.55 (6H, m), 7.42–7.31 (6H, m), 7.27–7.20 (2H, m), 4.58 (1H, s), 3.43 (4H, s), 2.85 (4H, s) ppm. ^{13}C{^{1}H} NMR (125 MHz, $(CD_3)_2CO$), 298 K) δ_C: 158.4, 158.2, 158.1, 153.3, 152.9, 152.8, 151.3, 149.7, 146.0, 138.9, 138.8, 136.7, 134.8, 132.4, 129.5, 129.3, 128.8, 128.7, 128.6, 127.2, 126.6, 125.3, 125.2, 117.7, 114.7, 76.9, 52.91 ppm. FTIR (solid, ATR) ν_{max} /cm^{-1}: 2922, 2851, 1618, 1603, 1447, 1423, 1377, 1227, 1134, 1007, 934, 827, 729, 556. UV–Vis (CD_3CN): λ_{max} /nm (ε/Lmol^{-1} cm^{-1}): 225 (40560), 246 (39220), 286 (57420), 342 (9560), 424 (10930), 452 (13140). HRMS (ES+): found *m/z* 422.1291, calculated *m/z* 422.1361 for $[C_{49}H_{42}N_8Ru]^{2+}$.

2.23. Synthesis of $[Ru(bipy)_2(L^8)](PF_6)_2$

$[Ru(bipy)_2Cl_2]$ (0.050 g, 0.1 mmol), **L^8** (0.070 g, 0.1 mmol) and $NaPF_6$ (0.038 g, 0.2 mmol) were combined in ethanol (5 mL). The mixture was degassed with N_2 for 20 min and heated to reflux for 72 h. The reaction was partially cooled and 0.1 M NH_4PF_6 (10 mL) was added. The precipitated was retrieved through filtration and washed with distilled water (3 × 5 mL) and diethyl ether (2 × 5 mL) to yield the product as an orange powder. (0.108 g, 96 %).^{1}H NMR (500 MHz, CD_3CN, 298 K) δ_H: 8.74 (1H, dd, J_{HH} = 8.5, 1.2 Hz), 8.53 (2H, dd, J_{HH} = 8.0, 3.5 Hz), 8.49 (2H, d, J_{HH} = 8.3 Hz), 8.44 (1H, dd, J_{HH} = 8.3, 1.1 Hz), 8.08 (2H, app. Ddd, J_{HH} = 8.1, 3.4, 1.3 Hz), 8.05 (1H, dd, J_{HH} = 5.2, 1.1 Hz), 8.01–7.96 (2H, m), 7.91 (1H, dd, J_{HH} = 5.2, 1.2 Hz), 7.86–7.81 (2H, m), 7.71 (1H, dd J_{HH} = 8.5, 5.2 Hz), 7.67 (1H, s), 7.63 (1H, dd, J_{HH} = 8.3, 5.2 Hz), 7.56 (2H, dd, J_{HH} = 6.7, 2.5 Hz), 7.45 (1H, dd, J_{HH} = 3.9, 1.5 Hz), 7.27–7.20 (2H, m), 5.40 (1H, d, J_{HH} = 5.1 Hz), 4.49–4.41 (1H, m), 3.75 (3H, s), 3.26 (1H, d J_{HH} = 12.3 Hz), 3.20 (4H, s), 2.43–2.27 (2H, m), 1.04 (3H, s), 0.93 (3H, d, J_{HH} = 6.5 Hz), 0.71 (3H, s) ppm. ^{13}C{^{1}H} NMR (101 MHz, CD_3CN, 298 K): δ_C: 158.2, 157.9, 155.8, 153.1, 152.9, 152.8, 151.4, 150.5, 149.7, 146.0, 141.1, 138.7, 138.6, 136.5, 134.5, 132.2, 129.4, 128.44, 128.43, 128.36, 128.3, 127.0, 126.4, 125.2, 125.1, 125.07, 123.2, 115.1, 75.9, 57.6, 57.0, 53.7, 51.0, 43.1, 40.2, 37.4, 36.9, 36.6, 28.9, 29.7, 24.4, 23.0, 22.8, 19.7, 19.1, 12.2 ppm. FTIR (solid, ATR) ν_{max} /cm^{-1}: 2945, 2868, 1695 (C═O carbamate), 1620, 1464, 1423, 1377, 1285, 1244, 1227, 1126, 1015, 835, 762, 731, 557. UV–Vis (MeCN): λ_{max} /nm (ε/Lmol^{-1} cm^{-1}): 226 (36240), 245 (40220), 255 (33170), 287 (65650), 340 (11310), 429 (13220), 451 (15460). HRMS (ES+) found *m/z* 545.2575, calculated *m/z* 545.2576 for $[C_{64}H_{76}N_8O_2Ru]^{2+}$.

3. Results and discussion

3.1. Synthesis and characterisation of the amine-functionalised ligands

A series of 1,10-phenanthroline (phen) based ligands were synthesized in two steps. Firstly, 5,6-epoxy-5,6-dihydro-1,10-phenanthroline was treated with either a morpholine, piperazine or piperidine derivative to give a 5,6-dihydro-1,10-phenanthroline-5-ol intermediate species (in the case of piperazine the intermediate is labelled **1** – see Scheme 3) that results from ring-opening of the epoxide group. These intermediate species (**1–7**) were fully characterised (see Experimental section for full details and SI for relevant spectra) with ^{1}H NMR spectra showing two doublet resonances noted at 4.0–5.5 ppm which were indicative of the protons at the 5,6-positions of the phenanthroline unit (i.e. confirmation of the 5,6-dihydro form of the ligand). The resultant loss of symmetry gave six unique proton environments around the phenanthroline ring, however, these resonances often overlapped in the aromatic region. The alteration of the aliphatic regions of the ^{1}H NMR spectra were consistent with the addition of the different amine derivatives in each case. The ^{13}C NMR spectra showed that the carbon environments associated with the 5,6-positions of the phenanthroline ring appeared ca. 65–70 ppm.

Treatment of **1**–**7** with NaH in dry THF resulted in the successful formation of the re-aromatized (and dehydrated) 5-amino substituted 1,10-phenanthroline compounds, **$L^{1–7}$**, in generally good yields. It is noteworthy, therefore, that **L^1** can be obtained without the need for mono-N-Boc protection of the piperazine [29]. Again, ^{1}H NMR spectra were especially informative highlighting the additional aromatic resonance at the 6-position of the phen species, together with retention of the relevant amine substituent in each case. The loss of the distinctive coupling patterns between 4 and 5 ppm (e.g. Fig. 1) that were evident in compounds **1**–**7** confirmed the re-aromatization of the products. ^{13}C{^{1}H} NMR also supported the transformation of the intermediates to the target ligands with the loss of the carbon signals at 65–70 ppm; because of the unsymmetrical nature of the ligands, overlapping peaks in the aromatic region were often observed. For the piperazine variants the aliphatic carbon resonances typically appeared around 50–55 ppm. In the case of **L^7** the benzyhydryl carbon was noted at 75.9 ppm. The presence of the CF_3 group in **L^5** allowed ^{19}F NMR data to be obtained revealing a singlet at −75.2 ppm. All species gave satisfactory HRMS data (see SI for all relevant data).

3.2. Synthesis and characterisation of the cholesterol variant, L^8

The utility of the piperazine-terminated ligand, **L^1**, was further demonstrated via a simple bioconjugation to give a cholesterol functionalized derivative. As part of our ongoing studies on the biological applications of photoluminescent metal complexes [30], we determined that the use of a cholesterol functionalised species may be of interest to a variety of targeted bioimaging studies in the future. There is precedent for cholesterol derivatives of metal complexes [31], and for Ru(II) a handful of examples have been reported. Firstly, a ligand based upon 5-amino-1,10-phenanthroline [32] to yield a complex for lipid bilayer studies; secondly, a monodentate thioether terminated ligand which can be photo-released from Ru(II) upon excitation to yield a cytotoxic product [33]; and thirdly, an ester-linked cholesterol adduct of a 2,2′-bipyridine ligand, which was reported during the course of our studies (Scheme 4) and used in plasma membrane imaging [34].

The synthesis of the cholesterol functionalised target ligand (**L^8**) was achieved using commercially available cholesteryl chloroformate. Thus, the use of an amine terminated ligand, such as **L^1**, allows covalent attachment of the cholesterol via a carbamate functional group. Carbamates are a well-known functional group often utilized within pharmaceutical agents implying good biocompatibility. The nature of the 'R' groups attached to the N and O atoms of the R-N-(C═O)-O-R' moiety can significantly alter the rate of hydrolysis [35] and thus stability of the carbamate. In general, more strongly electron donating R groups will increase the stability (both chemically, and enzymatically [36]) of the carbamate unit [37]; the chemical and biological stability of functionalised carbamates is an area of active research in medicinal chemistry [38]. Scheme 5 shows the synthetic route to **L^8** via the reaction of **L^1**, directly, with cholesteryl chloroformate in DCM [39] to yield the target ligand as a mustard yellow solid.

The key evidence for the transformation was provided by ^{1}H NMR spectral analysis with the loss of the singlet at 2.58 ppm due to the N*H* group in **L^1**, and the change in the appearance of the piperazine aliphatic signals at 3–4 ppm. The signature olefinic C*H* within the cholesteryl backbone was observed at 5.41 ppm, while the C═O resonance was observed in the ^{13}C NMR spectrum at 155 ppm. Furthermore, the

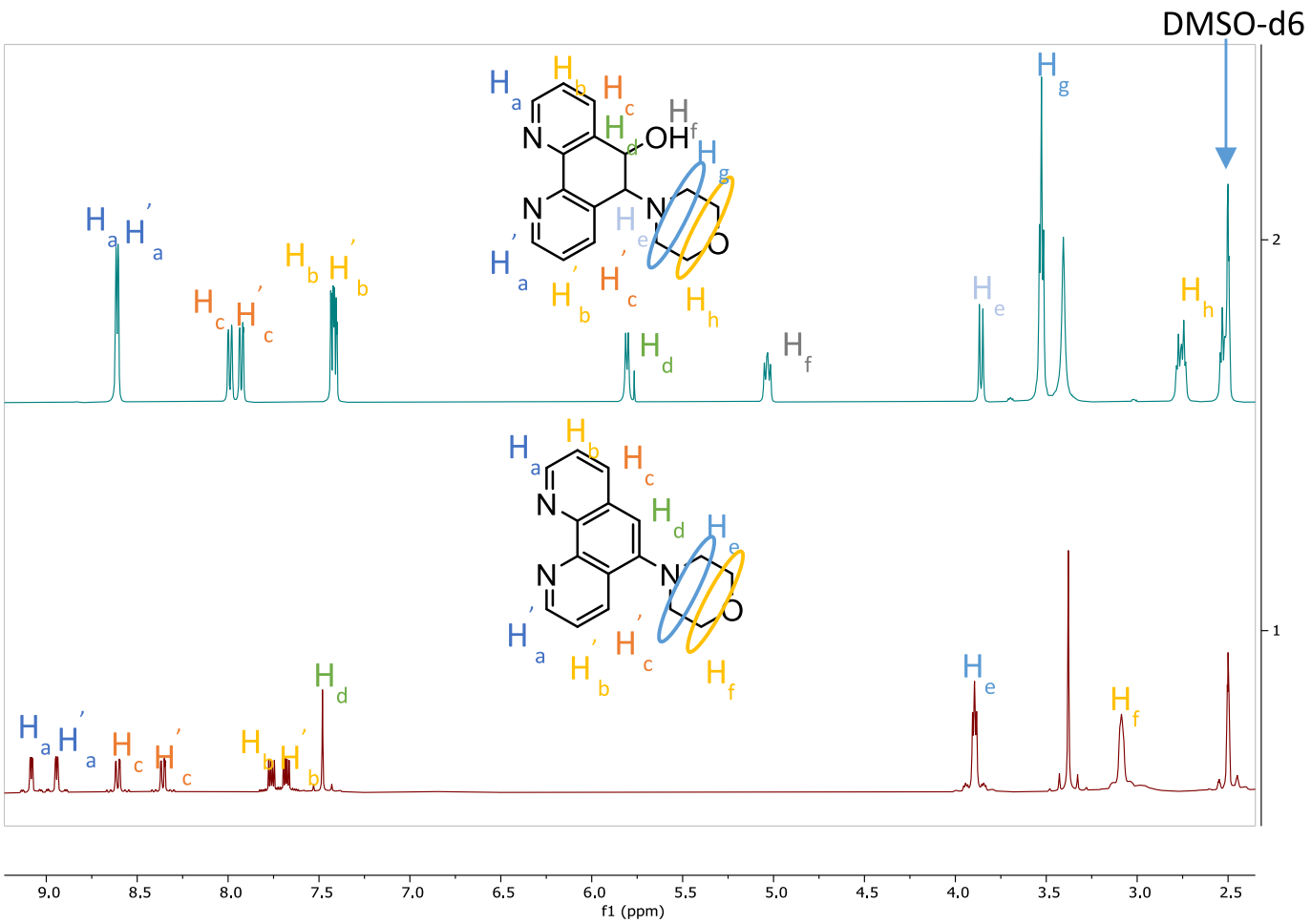

Fig. 1. A comparison of the ^{1}H NMR spectra for **2** and $\mathbf{L^2}$ showing the change in chemical shifts upon re-aromatisation.

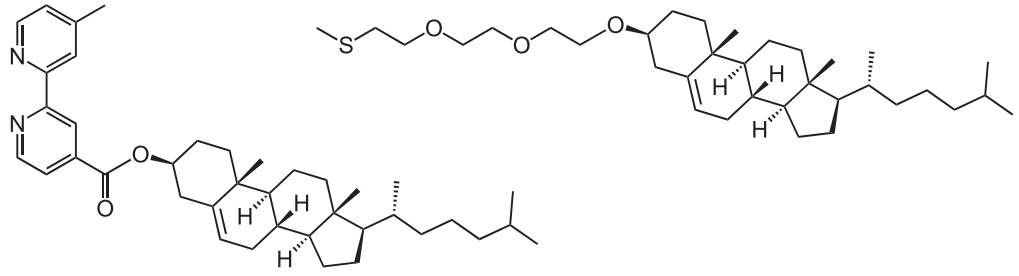

Scheme 4. Examples of cholesterol functionalised ligands reported for Ru(II): 2,2′-bipyridine (left) and thioether variants (right).

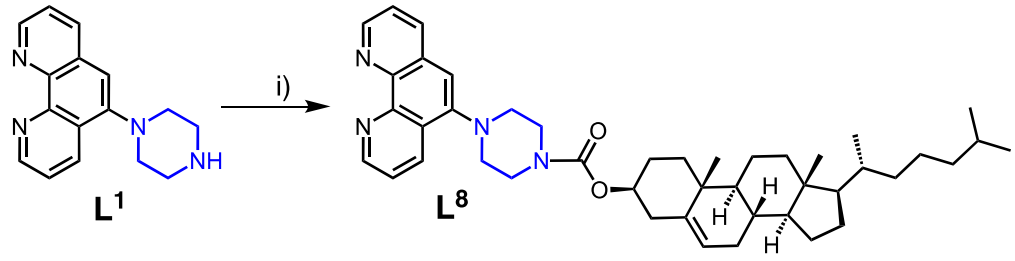

Scheme 5. Transformation of $\mathbf{L^1}$ to the cholesteryl derived ligand, $\mathbf{L^8}$. Reagents and conditions: i) cholesteryl chloroformate, dichloromethane.

formation of the carbamate group was also indicated by the IR spectrum with a strong stretch at 1692 cm^{-1} which indicates a slightly weaker C═O bond relative to the chloroformate (ca. 1780 cm^{-1}) starting material. A high resolution mass spectrum was obtained showing *m/z* 677.4800 which is consistent with $[M + H]^+$ for $\mathbf{L^8}$.

3.3. Synthesis of the Ruthenium Complexes

The coordination chemistry of Ru(II) is an excellent way to establish the behaviour of 1,10-phenanthroline ligands while yielding complexes with interesting electronic properties that can have potential in a variety of disciplines such as photoredox catalysis and bioimaging. Here, Ru(II) complexes were synthesized according to well established procedures: reaction of $[RuCl_2(bipy)_2]$ with stoichiometric ligand ($\mathbf{L^{1-8}}$) and $NaPF_6$ in refluxing EtOH resulted in the formation of red coloured solutions. After precipitation and filtration the complexes were isolated as orange coloured, air-stable solids in good yields. The formation of $[Ru(bipy)_2(\mathbf{L^{1-7}})](PF_6)_2$ was initially established using ^{1}H NMR spectroscopy. In each case the coordination of the unsymmetrical ligands $\mathbf{L^{1-7}}$ led to inequivalence in both of the 2,2′-bipyridine ligands and a correspondingly large number of aromatic resonances (in essence the signals are doubled). The aliphatic resonances associated with the phen substituent (piperazine, piperidine or morpholine groups) were also shown to subtly shift downfield upon coordination to Ru(II) with additional changes in the peak appearances. Similarly, the aromatic regions of the $^{13}C\{^1H\}$ NMR spectra were correspondingly complex with numerous overlapping resonances. In the case of $[Ru(bipy)_2(\mathbf{L^5})](PF_6)_2$ a ^{19}F NMR spectrum was obtained and showed two types of resonance at −74.3 (s) and − 72.9 (d,J_{FP} = 750 Hz) ppm, where the former is attributed to the CF_3 group and the latter is the PF_6^- counterion. Therefore, complexation of $\mathbf{L^5}$ induces a very subtle downfield shift compared to the free ligand (−75.2 ppm). All NMR spectra are presented in the SI.

HRMS were obtained in each case with *m/z* values consistent with either the di-cation [M – 2PF_6] and/or mono-cation [M – PF_6], each with the appropriate isotopic pattern for a ruthenium-containing species (Fig. 2). In the case of the benzyhydryl derivative, $[Ru(bipy)_2(\mathbf{L^7})](PF_6)_2$, an additional fragmentation was noted that related to the loss of the diphenylmethylene moiety from the ligand.

The cholesteryl ligand, $\mathbf{L^8}$, was reacted in an analogous manner to give $[Ru(bipy)_2(\mathbf{L^8})](PF_6)_2$ as an orange powder. While the resultant ^{1}H NMR spectrum featured numerous additional resonances in the aliphatic region, it was possible to identify features that confirmed chelation of $\mathbf{L^8}$ (e.g. downfield shift of the aliphatic protons within the bridging piperazine unit), and the presence of the cholesteryl unit (including an olefinic proton ca. 5.4 ppm). Comparison of the ^{13}C NMR data for $\mathbf{L^8}$ and its corresponding complex identify the carbamate carbonyl ^{13}C resonance around 155 ppm, in accordance with relevant literature on a related carbamate species [40]. Finally, the HRMS data for $[Ru(bipy)_2(\mathbf{L^8})](PF_6)_2$ was consistent with the identity of the double charged cation with *m/z* = 545.2575, showing that the cholesteryl moiety is covalently linked to the Ru(II) complex.

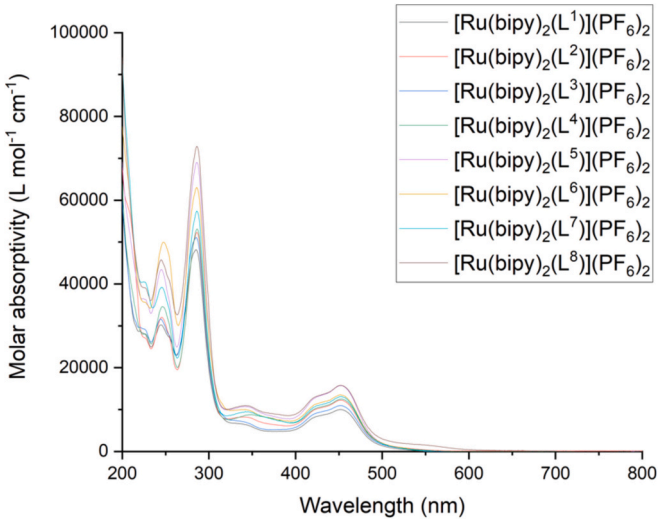

Fig. 2. UV–vis. Spectra for the series of ruthenium complexes (293 K, aerated MeCN).

Electronic properties of the ligands and complexes

Solutions of the ligands display electronic absorption spectra that reveal strong absorptions in the UV region that relate to allowed π → π* transitions; in each case three bands were observed between 200 and 325 nm (typically ε > 10^4 M^{-1} cm^{-1}), consistent with an amine-substituted 1,10-phenanthroline chromophore. The UV–vis absorption data (Table 1) for the complexes $[Ru(bipy)_2(\mathbf{L^{1-8}})](PF_6)_2$ revealed strong similarities with the benchmark compound $[Ru(bipy)_3]^{2+}$ [1]. Intense ligand-centred bands, which are subtly perturbed upon coordination and now a composite of bipy-centred transitions (particularly noted around 290 nm) and those attributed to $\mathbf{L^{1-8}}$, were observable between 200 and 350 nm. A new broader band was now evident at 400–500 nm which is attributed to the spin-allowed^{1}MLCT transition (λ_{max} ~ 452 nm; ε ~ 10^4 M^{-1} cm^{-1}) (see Fig. 2) that is classically observed for polypyridine complexes of Ru(II) [1]. The band envelope (and associated vibronic progressions) appears consistent across the series of complexes. The variations in the nature of the substituent (piperazine, piperidine, morpholine based) at the 1,10-phenanthroline ligand do not induce any notable variations within the series of complexes, and further functionalisation with the cholesteryl functionalized complex possesses the same efficient absorption in the visible region.

The luminescence properties of the complexes were also assessed under both aerated and deoxygenated conditions (Table 1). As expected, following excitation at the ^{1}MLCT band each complex showed a broad featureless peak centred around 605–610 nm, which is typical of a ^{3}MLCT emission [1]. The emission profiles are essentially superimposable (Fig. 3) showing how the intrinsic electronic properties are not influenced by the different ligand peripheries. Quantum yield values were also typical of complexes of this type under aerated conditions (1.8–5.0 %); slightly higher values were noted for $[Ru(bipy)_2(\mathbf{L^6})](PF_6)_2$ and $[Ru(bipy)_2(\mathbf{L^7})](PF_6)_2$ and this may be due to the larger phenyl substituents, that are present at the ligand periphery, that may offer a small degree of shielding from diffusing oxygen. Upon degassing the values increase to ca. 6.2–8.8 % which again is consistent with benchmark compounds such as $[Ru(bipy)_3][PF_6]_2$.

The associated experimental lifetimes, obtained from fitting the decay traces via time resolved measurements (λ_{ex} = 295 nm) were

Table 1
Photoluminescence data for the family of Ru(II) complexes.[a]

Complex	Emission λ / nm[b]	Lifetime τ / μs[c]	Quantum yield Φ [d]	k_r / s^{-1}	k_{nr} / s^{-1}
$[Ru(bipy)_2(\mathbf{L^1})][PF_6]_2$	605	0.15 (0.77)	0.018 (0.076)	9.87 × 10^4	1.20 × 10^6
$[Ru(bipy)_2(\mathbf{L^2})][PF_6]_2$	606	0.14 (0.84)	0.019 (0.088)	1.05 × 10^5	1.09 × 10^6
$[Ru(bipy)_2(\mathbf{L^3})][PF_6]_2$	605	0.14 (0.76)	0.018 (0.072)	9.47 × 10^4	1.22 × 10^6
$[Ru(bipy)_2(\mathbf{L^4})][PF_6]_2$	608	0.15 (0.73)	0.026 (0.078)	1.07 × 10^5	1.26 × 10^6
$[Ru(bipy)_2(\mathbf{L^5})][PF_6]_2$	610	0.15 (0.84)	0.016 (0.083)	9.88 × 10^4	1.09 × 10^6
$[Ru(bipy)_2(\mathbf{L^6})][PF_6]_2$	610	0.14 (0.54)	0.050 (0.062)	1.15 × 10^5	1.74 × 10^6
$[Ru(bipy)_2(\mathbf{L^7})][PF_6]_2$	608	0.15 (0.81)	0.047 (0.081)	1.00 × 10^5	1.13 × 10^6
$[Ru(bipy)_2(\mathbf{L^8})][PF_6]_2$	607	0.15 (0.79)	0.018 (0.079)	1.00 × 10^5	1.17 × 10^6

[a] All measurements obtained in MeCN at 293 K. [a] 3.33 × 10^{-6} M solutions in aerated MeCN; [b] maximal phosphorescence emission wavelength; [c] aerated phosphorescence lifetimes; values in parentheses are degassed; [d] phosphorescence quantum yields (λ_{ex} = 450 nm); using $[Ru(bipy)_3][PF_6]_2$ in aerated MeCN (Φ = 0.018) in degassed MeCN (values in parentheses) as a reference (Φ = 0.095), errors are estimated at 15 %. Estimates of k_r and k_{nr} from degassed data using $k_r = \Phi/\tau$ and $k_{nr} = (1 - \Phi)/\tau$.

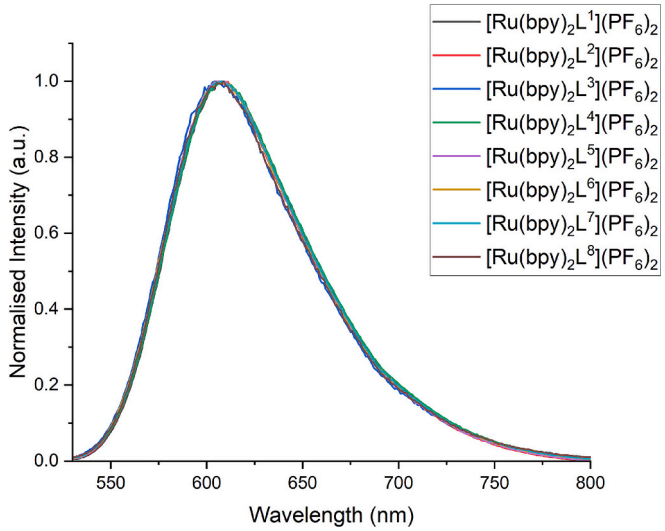

Fig. 3. Normalised emission spectra for the series of ruthenium complexes (293 K, aerated MeCN, λ_{ex} = 450 nm).

typically around 0.14–0.15 μs in aerated MeCN while degassing led to significant increases to 0.54–0.84 μs. Therefore the photophysical data fully supports the assignment that these are phosphorescent ^{3}MLCT emitters (and demonstrably sensitive to molecular oxygen as a quencher) which are closely analogous to $[Ru(bipy)_3](PF_6)_2$. Again, across the series of complexes the nature of the substituents at the ancillary ligand induces very little perturbation of the excited state character. This is particularly notable for the piperazine substituted systems where the presence of the bridging amine does not lead to any notable quenching (via photoinduced electron transfer) of the excited state of the complex. Importantly, functionalization with the cholesteryl moiety does not compromise the desirable ^{3}MLCT photophysical properties of the Ru(II) complex. This suggests that this red-emitting complex should be of significant interest for cellular bioimaging studies in the future, including studies into cholesterol intracellular trafficking experiments.

4. Conclusions

The use of 5,6-epoxy-5,6-dihydro-1,10-phenanthroline as a precursor is a very convenient approach for accessing a wide range of amine-substituted ligands with varying functionality. The synthetic methodology allows ligands to be isolated over two steps and shows that morpholine, piperazine, and piperidine derivatives are all tolerant to the reaction protocols. Furthermore, the use of piperazine allows the development of ligands for further functionalisation, and very recent studies have shown interesting precedent for peptide coupling using a piperazine spacer on related Ir(III) complexes for bioimaging [27]. In this case, it was demonstrated that the ligand can be easily bioconjugated using a cholesterol chloroformate derivative. Importantly, the variation in functionalisation does not lead to any compromise with regard to the ^{3}MLCT photophysical properties of the Ru(II) complexes reported herein. Such a straightforward synthetic approach should be of interest to those who are engaged in the development of luminescent metal complexes for different optoelectronic applications.

Tools for probing intracellular sterol dynamics can provide an important approach for investigating many cellular functions [41]. Luminescent sterols are one approach to be exploited in an area of active research [42]. Our future studies will investigate the biological utility of cholesterol functionalised $[Ru(bipy)_2(\mathbf{L^8})](PF_6)_2$, including cellular studies for specific disease states where cholesterol trafficking is important. This complex marries significant photophysical advantages for cell imaging (visible excitation, long wavelength emission, large Stokes' shift, and long luminescence lifetime) with targeted bioconjugation and should provide an interesting entry point for future studies.

Declaration of competing interest

The authors declare that they have no known competing financial interests or personal relationships that could have appeared to influence the work reported in this paper.

Acknowledgements

We would like to thank EPSRC for funding the PhD studentship of AIB (grant code: EP/L504749/1).

Appendix A. Supplementary data

Supplementary data to this article can be found online at https://doi.org/10.1016/j.ica.2025.122561.

Data availability

The data in this study are available at the Cardiff University data repository https://doi.org/10.17036/cardiff.28270598.

References

[1] A. Juris, V. Balzani, F. Barigelletti, S. Campagna, P. Belser, A. von Zelewsky, Coord. Chem. Rev. 84 (1988) 85.
[2] H. Yersin, D. Braun, Coord. Chem. Rev. 111 (1991) 39.
[3] (a) J.V. Caspar, T.J. Meyer, J. Am. Chem. Soc. 105 (1983) 5583;
(b) O.S. Wenger, Coord. Chem. Rev. 282 (282) (2015) 150.
[4] (a) E.T. Luis, H. Iranmanesh, J.E. Beves, Polyhedron 160 (2019) 1;
(b) D.C. Fabry, M. Reuping, Acc. Chem. Res. 49 (2016) 1969;
(c) T. Koike, M. Akita, Inorg. Chem. Front. 1 (2014) 562.
[5] (a) J.D. Bell, J.A. Murphy, Chem. Soc. Rev. 50 (2021) 9540;
(b) S. Angerani, N. Winssinger, Chem. Eur. J. 25 (2019) 6661;
(c) K. Teegardin, J.I. Day, J. Chan, J. Weaver, Org. Process Res. Dev. 20 (2016) 1156;
(d) Y.-L. Li, A.-J. Li, S.-L. Huang, J.J. Vittal, G.-Y. Yang, Chem. Soc. Rev. 52 (2023) 4725.
[6] (a) For example G. Li, L. Sun, L. Ji, H. Chao, Dalton Trans. (2016) 45;
(b) A.E. Friedman, J.C. Chambron, J.-P. Sauvage, N.J. Turro, J.K. Barton, J. Am. Chem. Soc. 112 (1990) 4960.
[7] (a) L.K. McKenzie, H.E. Bryant, J.A. Weinstein, Coord. Chem. Rev. 379 (2019) 2;
(b) O.J. Stacey, S.J.A. Pope, RSC Adv. 3 (2013) 25550.
[8] (a) F. Heineman, J. Karges, G. Gasser, Acc. Chem. Res. 50 (2017) 2727;
(b) E. Wachter, D.K. Heidary, B.S. Howerton, S. Parkin, E.C. Glazer, Chem. Commun. 48 (2012) 9649.
[9] (a) S. Bonnet, J. Am. Chem. Soc. 145 (2023) 23397;
(b) C.E. Elgar, N.A. Yusoh, P.R. Tilley, N. Kolozsvari, L.G. Bennett, A. Gamble, E. V. Pean, M.L. Davies, C.J. Staples, H. Ahmad, M.R. Gill, J. Am. Chem. Soc. 145 (2023) 1236.
[10] (a) B.K. Pragti, S. Kundu, Mukhopadhyay, Coord. Chem. Rev. 448 (2021) 214169;
(b) K.T. McQuaid, C.J. Cardin, Med. Chem. 75 (2020) 393.
[11] (a) L.C.-C. Lee, K.K.-W. Lo, Chem. Rev. (2024), https://doi.org/10.1021/acs.chemrev.3c00629;
(b) V. Fernandez-Moreira, F.L. Thorp-Greenwood, M.P. Coogan, Chem. Commun. 46 (2010) 186;
(c) L.C.C. Lee, K.K.W. Lo, Chem. Asian J. 17 (17) (2022) e202200840;
(d) F.E. Poynton, S.A. Bright, S. Blasco, D.C. Williams, J.M. Kelly, T. Gunnlaugsson, Chem. Soc. Rev. 46 (2017) 7706;
(e) G.X. Xu, E.C.L. Mak, K.K.W. Lo, Inorg. Chem. Front. 8 (2021) 4553.
[12] (a) For example P.G. Sammes, G. Yahioglu, Chem. Soc. Rev. 23 (1994) 327;
(b) A. Bencini, V. Lippolis, Coord. Chem. Rev. 254 (2010) 2096;
(c) P. Alreja, N. Kaur, RSC Adv. 6 (2016) 23169.
[13] C. Queffelec, P.B. Pati, Y. Pellegrin, Chem. Rev. 124 (2024) 6700.
[14] (a) N.M. Shavaleev, H. Adams, J.A. Weinstein, Inorg. Chim. Acta 360 (2007) 700;
(b) R.O. Bonello, M.B. Pitak, G.J. Tizzard, S.J. Coles, I.A. Fallis, S.J.A. Pope, Polyhedron 228 (2022) 116179.
[15] (a) A.W. McKinley, P. Licoln, E.M. Tuite, Coord. Chem. Rev. 255 (2011) 2676;
(b) M.L. Di Pietro, G. La Ganga, F. Nastasi, F. Puntoreiro, Appl. Sci. 11 (2021) 3038.
[16] (a) For example S. Kumar, S. Singh, A. Kumar, K.S.R. Murthy, A.K. Singh, Coord. Chem. Rev. 452 (2022) 214272;
(b) R.O. Bonello, I.R. Morgan, B.R. Yeo, L.E.J. Jones, B.M. Kariuki, I.A. Fallis, S.J. A. Pope, J. Organomet. Chem. 749 (2014) 150;
(c) R.O. Bonello, M.B. Pitak, S.J. Coles, A.J. Hallett, I.A. Fallis, S.J.A. Pope,

J. Organomet. Chem. 841 (2017) 39;
(d) E.E. Langdon-Jones, B.D. Ward, S.J.A. Pope, J. Organomet. Chem. 861 (2018) 234;
(e) E.M. Regan, A.J. Hallett, L.C.C. Wong, I.Q. Saeed, E.E. Langdon-Jones, N. J. Buurma, S.J.A. Pope, P. Estrela, Electrochim. Acta 128 (2014) 10.
[17] S. Krishnan, D.G. Kuhn, G.A. Hamilton, J. Am. Chem. Soc. 99 (1977) 8121.
[18] (a) N.K. Shee, M.G.B. Drew, D. Datta, New. J. Chem. 41 (2017) 452;
(b) V. Komreddy, K. Ensz, H. Nguyen, D.P. Rillema, C.E. Moore, J. Mol. Struct. 1223 (2021) 128739.
[19] I.A. Dotsenko, M. Curtis, N.M. Samoshina, V.V. Samoshin, Tetrahedron 67 (2011) 7470.
[20] E. Rousset, O. Mongin, J. Moreau, L.M. Lawson-Daku, M. Beley, P.C. Gros, S. Chevreux, M. Blanchard-Desce, G. Lemercier, Dalton Trans. 50 (2021) 10119.
[21] (a) M. Riklin, D. Tran, X. Bu, L.E. Laverman, P.C. Ford, J. Chem. Soc., Dalton Trans. (2001) 1813;
(b) M.M. Lezhnina, D. Hoffmann, B. Santiago-Schubel, P. Klauth, U.H. Kynast, New J. Chem. 36 (2012) 2322.
[22] S. Dwaraknath, N.-H. Tran, T. Dao, A. Colbert, S. Mullen, A. Nguyen, A. Cortez, L. Cheruzel, J. Inorg. Biochem. 136 (2014) 154.
[23] W. Wang, K. Vellaisamy, G. Li, C. Wu, C.-N. Ko, C.-H. Leung, D.-L. Ma, Anal. Chem. 89 (2017) 11679.
[24] V. Shen, B.P. Sullivan, Inorg. Chem. 34 (1995) 6235.
[25] J. Paris, C. Gameiro, V. Humbleyt, P.K. Mohapatra, V. Jacques, J.F. Desreux, Inorg. Chem. 45 (2006) 5092.
[26] M. Ahmadi, S. Seiffert, Macromol 54 (2021) 1388.
[27] T. Lauria, C. Slator, V. McKie, M. Muller, S. Stazzoni, A.L. Crisp, T. Carell, A. Kellett, Chem. Eur. J. 26 (2020) 16782.
[28] H. Ishida, S. Tobita, Y. Hasegawa, R. Katoh, K. Nozaki, Coord. Chem. Rev. 254 (2010) 2449.
[29] M. Yasukagawa, A. Shimada, S. Shiozaki, S. Tobita, T. Yoshihara, Sci. Rep. 11 (2021) 4733.
[30] (a) For example A.H. Day, M.H. Übler, H.L. Best, E. Lloyd-Evans, R.J. Mart, I. A. Fallis, R.K. Allemann, E.A.H. Al-Wattar, N.I. Keymer, N.J. Buurma, S.J.A. Pope, Chem. Sci. 11 (2020) 1599;
(b) A.H. Day, J. Domarkas, S. Nigam, I. Renard, C. Cawthorne, B.P. Burke, G. S. Bahra, P.C.F. Oyston, I.A. Fallis, S.J. Archibald, S.J.A. Pope, Dalton Trans. 49 (2020) 511;
(c) L.M. Groves, C.F. Williams, A.J. Hayes, B.D. Ward, M.D. Isaacs, N.O. Symonds, D. Lloyd, P.N. Horton, S.J. Coles, S.J.A. Pope, Dalton Trans. 48 (2019) 1599.
[31] (a) For example G. Vitiello, A. Luchini, G. D'Errico, R. Santamaria, A. Capuozzo, C. Irace, D. Mentesarchio, L. Paduano, J. Mat. Chem. B 3 (2015) 3011;
(b) K. Kawaguchi, T. Seki, T. Karatsu, A. Kitamura, H. Ito, S. Yagai, Chem. Commun. 49 (2013) 11391.
[32] A. Sharmin, L. Salassa, E. Rosenberg, J.B.A. Ross, G. Abbott, L. Black, M. Terwilliger, R. Brooks, Inorg. Chem. 52 (2013) 10835.
[33] B. Siewart, V.H.S. van Rixel, E.J. van Rooden, S.L. Hopkins, M.J.B. Moester, F. Ariese, M.A. Siegler, S. Bonnet, Chem. Eur. J. 22 (2016) 10968.
[34] Q. Fa, X.A. Gao, W.Z. Zhang, J.Y. Ren, B. Song, J.L. Yuan, Inorg. Chem. 63 (2024) 10443.
[35] L.W. Dittert, T. Higuchi, J. Pharm. Sci. 52 (1963) 852.
[36] A. Mattarei, M. Azzolini, M. La Spoina, M. Zoratti, C. Paradisi, L. Biasutto, Sci. Rep. 5 (2015) 15216.
[37] F. Vacondio, C. Silva, A. Lodola, A. Fioni, S. Rivara, A. Duranti, A. Tontini, S. Sanchini, J.R. Clapper, D. Piomelli, M. Mor, G. Tarzia, ChemMedChem 4 (2009) 1495.
[38] A.K. Ghosh, M. Brindisi, J. Med. Chem. 58 (2015) 2895.
[39] S. Malik, S.I. Kawano, N. Fujita, S. Shinkai, Tetrahedron 63 (2007) 7326.
[40] R. Ul Islam, M.M. Johnson, R. Mohammed, J. Hean, P. Arbuthnot, C.B. de Koning, W.A.L. van Otterlo, S. Afr. J. Chem. 63 (2010) 88.
[41] B. Mesmin, F.R. Maxfield, Biochimica et Biophysica Acta 1791 (2009) 636.
[42] (a) F.R. Maxfield, D., Wustner *Analysis of cholesterol trafficking with fluorescent probes* in *Methods in Cell Biology*, Elsevier, 2012;
(b) K.A. Solanko, M. Modzel, L.M. Solanko, D. Wustner, Lipid Insights 8 (2015) 95;
(c) D. O'Connor, A. Byrne, T.E. Keyes, RSC Adv 9 (2019) 22805;
(d) A. Maiwald, O. Bauer, G. Gimpi, Biochimica et Biophysica Acta 1859 (2017) 1099.